ELSEVIER

Nuclear Instruments and Methods in Physics Research B 152 (1999) 449–458

NIM B
Beam Interactions with Materials & Atoms

www.elsevier.nl/locate/nimb

Crystal order near the point of impact under static keV ion bombardment

Che-Chen Chang

Department of Chemistry, National Taiwan University, Taipei, Taiwan

Received 27 July 1998; received in revised form 12 January 1999

Abstract

The surface damage created by static bombardment of keV ions is investigated using the Ag surface as a model system. Results from molecular dynamics calculations show that the sputtering events induced by the static ion beam take place in the sub-ps time range. Studies on the property of the underlayer atoms which eject late in the collision cascade reveal that in this time range the lattice structure of the surface in the impact region is not severely disrupted by the impinging ion. The degree of the structural disturbance in the surface after atom sputtering is evaluated by calculating the average and the most probable distances of displacement of the residual atoms from their lattice sites. Most surface atoms in the impact region are displaced by only a fraction of the equilibrium bond length in the solid after the ion bombardment, although the distance of displacement may be larger than the Lindemann radius. The displacement does not increase monotonously with the size or the energy of the impinging ion. The dependence of the extent of surface damage upon the initial distance of the surface atom from the target atom is quantitatively determined. The extent of the structural destruction in the surface decreases rapidly with increasing initial distances of the surface atoms from the target atom. The surface order after the static ion bombardment is related to the density of the surface atoms exposed to the incident ions. The average distance of displacement calculated from the Ag{1 1 0} surface is about 0.2 lattice spacings smaller than those obtained from the Ag{1 0 0} and the Ag{1 1 1} surfaces. Applications of these results to the structural determination of surfaces using the static secondary ion mass spectrometry are discussed.

1. Introduction

The degree of control possible with an ion beam has made dry etching by ion bombardment a powerful technique for fabricating electronic and optoelectronic structures on the nanometer scale [1–5]. Since high quality electronic devices are usually produced on clean and undamaged substrates, the full utilization of the ion-beam technique in fabricating devices thus relies upon a better understanding at the atomic level of the generation and the propagation of the surface damage introduced by the ion impact [6–10]. Experimental studies showed that the impingement of energetic ions on a crystal surface may effect the formation of vacancies [11–13], craters [14,15], adatom islands [16], gas bubbles [17], dislocation loops [18,19], amorphous layers [20], and the structural disorder [21]. In addition, stacking faults and atomic displacement and migration

0168-583X/99/$ – see front matter
PII: S0168-583X(99)00177-9

[14,15,22,23] may also occur under energetic ion bombardment. Theoretical modeling [24,25] of the ion-surface collision event revealed that considerable surface damage may be created if the primary knockons remained in the top few atomic layers of the surface long enough such that sufficient momentum could be imparted in the upper surface layers to produce sputtering and lattice distortion. Based on the analysis of the collision cascade induced by the ion impact and of the maximum lateral separation of the sputtered atoms, it was found that some damages, such as those created in the so-called "mega-events", might be spread laterally for a distance of the order of a hundred Angstroms or more [24,25].

Instead of focusing on the isolated events or special types of surface damage, we will concentrate in this paper on the overall damage of the metal surface induced by static bombardment of energetic ions [26–31]. In particular, the structural disruption created due to the dissipation of ion energy in the surface near the point of impact will be investigated. The macroscopic quantities observed experimentally represent results of an ensemble effect exerted on the surface during ion bombardment. Factors such as the surface temperature, the propagation of momentum through collisions, and the interaction among the collision cascades initiated by different incident ions may all play some roles in determining the final state of the ion-bombarded surface. Information about the effect of the ion collision on the creation of surface damage cannot be easily extracted without resorting to the theoretical calculation. By theoretically separating the collision event from the thermal effect and from the events occurring due to the cascade mixing, one may be able to better predict the exact role of the ion impact in the damage formation on the surface.

In this study, the effect of static ion bombardment on the surface structure will be evaluated by examining the dependence of surface damage upon the initial distance (i.e., the distance before the ion impact), from the impact point, of the atoms in the surface. The most probable atomic displacement, the average displacement, and the functional relationship between the average distance of displacement and the distance of the initial atomic location from the point of impact will be calculated in order to quantitatively estimate the degree of the surface damage introduced by the impact of individual ions. Furthermore, the effects of both the kinetic energy and the size of the bombarding ion on the degree of surface damage will be studied. The extent of the structural disturbance induced by the single-ion impacts is found to be related to the number of atoms per unit area of the surface exposed to the incident ion beam.

2. Computational method

The final state of the surface is determined in this study using a classical dynamics procedure to calculate the development of the collision cascades which are initiated by the static ion bombardment. The detail of the procedure [32,33] has been described previously. Three Ag crystallites of different low-index faces are used in this study. The sizes of the model crystallites required for the calculation are tested separately for each face and for different incident energies. Results of the tests show that for 1 keV Ar ions incident on different faces, the crystallites consisting of at least 7 atomic layers with more than 350 atoms per layer are required to contain the motion of all the atoms originally residing within 4 lattice spacings (LS, 1 LS = 4.086 Å) from the target atom. This atom is selected in this study as the first-layer atom in the impact zone. The initial temperature of the crystallite is set to be zero Kelvin such that all the atomic motion occurring in the surface is induced by the bombardment of the incident ion only.

These crystallites are then subjected to ion bombardment at normal incidence. On each crystallite, as many as 1600 ions are allowed to impinge uniformly and statically on a zone of irreducible surface symmetry [34]. The dissipation of momentum which results when an energetic ion impinges on the surface is then predicted by integrating Hamilton's equations of motion. It allows the positions and momenta of all the particles to be determined as a function of time during ion bombardment. The collision cascade is terminated when the momentum carried by the incident ion has been dissipated throughout the model crys-

tallite. In practice, the calculation is stopped when no surface atoms are more energetic than 0.2 eV and the incident ion has an energy of less than one-thousand of the primary energy. The final positions and velocities of all the surface atoms are then used to study the state of the surface after ion bombardment.

The nature of the ion–surface interaction potential is assumed to be a Moliere type [35], with the Thomas–Fermi screening length adjusted according to the Firsov model [36] and O'Connor's formula [37]. In addition, atoms in the crystal are allowed to interact with each other according to the pairwise additive forces derived from the Morse potential [38–40]. The interaction of these atoms vanishes smoothly at a distance greater than the one corresponding to the separation of the second nearest neighbors. At small distances, the interaction of surface atoms is described by the Moliere potential, which is fitted by a cubic spline to the Morse potential at a distance around half the separation of the first nearest neighbors.

3. Results and discussion

The extent of the surface damage induced by ion bombardment may be explored by examining the ejection behavior of the atoms sputtered from below the topmost atomic layer of the surface. For a surface in which much of the crystal order is destroyed during ion bombardment, the underlayer atoms may eject from the surface with about an equal probability through different points in the plane of the topmost atomic layer. In other words, the take-off points of the underlayer atoms ejecting from a severely disrupted surface should be almost uniformly distributed in the plane of the topmost layer around both the lattice site and the lattice hole within the region near the point of the ion impact. Furthermore, atoms ejecting late in the collision cascade should experience a surface which is more damaged than those ejecting early in the cascade. Fig. 1 shows the distribution of the time intervals (the so-called ejection times) between the instant of the primary ion impact and the moments at which ejecting atoms leave the surface due to the impact of the primary ion. The

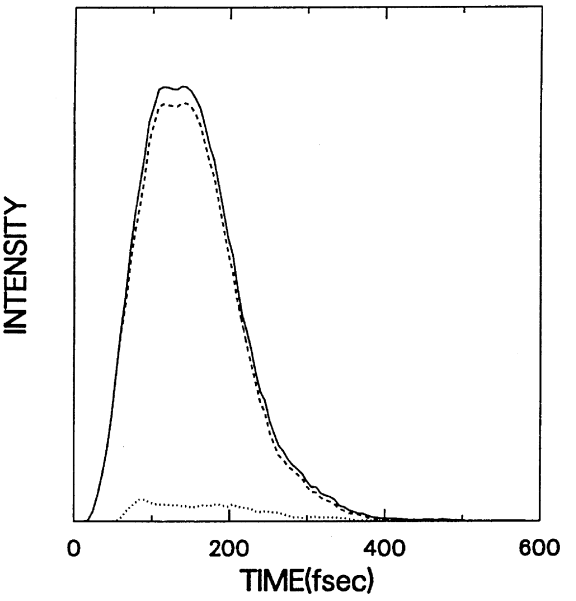

Fig. 1. Calculated distribution of the time intervals between the instant of the ion impact and the moments in which surface atoms take off from the Ag{1 0 0} surface due to bombardment of 600 eV Ar^+ ions normal to the surface. The total number of ion impacts is 1600. The solid curve represents the distribution for all the atoms sputtered from the surface; the dashed curve the one from the first atomic layer; the dotted line the one from the second layer.

moment an ejecting atoms leaves the surface is defined in this study as the instant this atom moves past the potential cutoff distance from its nearest neighbor. For the case of a Ag atom ejecting from the Ag surface, this distance is arbitrarily chosen to be 1.2 LS. As shown in Fig. 1, the sputtering of atoms from the Ag{1 0 0} surface by the 600 eV Ar^+ ions mostly takes place in the sub-ps time range after the primary ion impact. Atoms may take off from the surface at an ejection time as short as 20 fs after the ion impact. Analysis of the sputtering process indicates that most of these short-ejection-time atoms originate from the topmost layer. The ejection-time distribution has a peak time at $\sim$125 fs. A few atoms may eject very late in the cascade with ejection times as large as more than 500 fs. Fig. 1 also shows the ejection-time distributions of the sputtered atoms originating from the first and the second atomic layers, respectively. Atoms ejecting from the second-layer

have a smaller ejection-time range than those from the first-layer. The earliest ejection of the second-layer atom occurs at ~50 fs after the ion impact and the latest ejection occurs at ~480 fs.

With the understanding of the ejection-time distribution of the atoms sputtered from the surface, the ejection property of the atoms taking off late in the collision cascade can then be investigated. Shown in Fig. 2 is the distribution of the take-off points, located in the plane of the first atomic layer, through which the second-layer atoms move up and then eject from the Ag{1 0 0} surface. Only the take-off points of the atoms which leave the surface at time intervals of more than 320 fs after the ion impact are plotted. The distribution thus contains information about the ejection behavior of all the second-layer atoms which leave the surface late in the collision cascade when the surface disruption is most severe. However, the figure shows that, instead of being uniformly distributed about both the lattice sites and the holes, the take-off points are mainly located in the fourfold holes of the {1 0 0} surface. It appears that the first-layer atoms are able to confine the path of the emitting second-layer atoms to some extent late in the cascade.

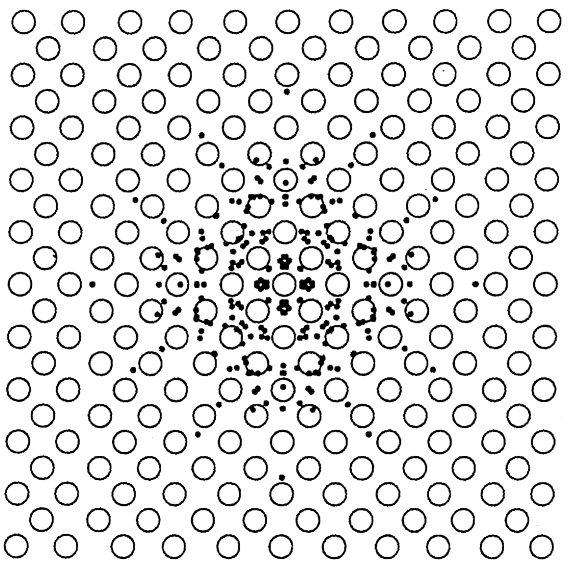

Fig. 2. The calculated distribution of the take-off points in the plane of the topmost surface layer for atoms originating from the second layer of the Ag{1 0 0} surface and emitting to all angles with ejection times of between 320 and 370 fs. The incident Ar^+ ion has a kinetic energy of 600 eV and is at normal incidence onto an impact zone of irreducible surface symmetry located near the center of the plot. The total number of ion impacts is 1600. The open circles represent surface atoms in the first layer and the small closed circles the take-off points.

The atoms which eject late in the collision cascade generally have very low kinetic energy [40]. Our studies of the relationship between the ejection time and the kinetic energy of ejection indicate that very few atoms with kinetic energies of more than 8 eV eject out of the surface at time intervals of more than 320 fs after the primary impact. Time-exposure cascade analysis [41,42] reveals that some of the low-energy second-layer atoms which contribute to the take-off point distribution shown in Fig. 2 may travel in the space between the top two atomic layers for as far as more than 2 LS before they are scattered out of the surface. Since atoms with low momenta are prone to deflection during their traveling in the surface, the appearance of the take-off points of most ejecting second-layer atoms in the fourfold holes of the first atomic plane indicates that at the later stage of the collision cascade for sputtering, most of the first-layer atoms surrounding the fourfold holes are not displaced far away from their initial lattice sites. The fact that most of the second-layer atoms which eject from within 3 LS of the impact point, where the most severe structural disruption is expected, are able to be somewhat constrained to emit through the lattice holes thus reveals that the surface retains to a certain extent the initial crystal order in the time range of this study during static ion bombardment. We note that near the end of the collision cascade for sputtering, some first-layer atoms may have been sputtered from the surface and others may be displaced to various orientations. The take-off points of the second-layer atoms shown in Fig. 2 are thus not concentrated around the center of the lattice hole.

The state of the surface is then studied by examining, after ion bombardment, the magnitude of displacement of the residual surface atoms from their initial lattice sites. Presented in Fig. 3 are the displacement distributions of the atoms remaining in the surface which are initially located within 4 LS from the target atom. These distributions are

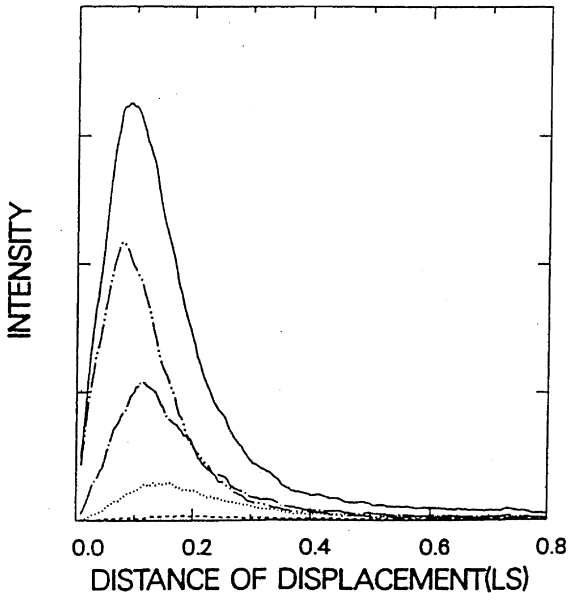

Fig. 3. Displacement distributions of the atoms remaining in the Ag{1 0 0} surface after the surface is bombarded by Ar^+ ions of 600 eV incident energy. The distributions are comprised of the effects of 100 individual ion impacts distributed uniformly in an impact zone of irreducible surface symmetry. Only the distances of displacement of the atoms initially residing within 4 LS from the target atom are included. The solid curve represents the distribution of the displacement from the lattice site for the atoms initially residing within 4 LS from the target atom. The dashed curve represents the displacement distribution for the atoms initially residing within 1 LS; the dotted line the one residing between 1 and 2 LS; the dot-dashed line the one residing between 2 and 3 LS; and the dot-dot-dashed line the one residing between 3 and 4 LS.

obtained by averaging over all the damages created by 100 individual ion impacts which are distributed uniformly in a zone of irreducible surface symmetry [39]. The overall distribution (solid curve) has a peak distance of displacement, i.e. the most probable distance of displacement, at about 0.09 LS (or 0.37 Å) from the initial lattice site. It indicates that the static bombardment of the 600 eV Ar^+ ions on the Ag{1 0 0} surface causes most of the surface atoms around the impact point to move by about one eighth of the equilibrium Ag–Ag bond length (2.889 Å) in the solid. In fact, integrating the area under the curve of Fig. 3 reveals that, in the sub-ps time range of this study, more than 90% of the residual surface atoms which initially reside within 4 LS from the target atom are displaced with a distance of less than half of the equilibrium bond length in the bulk.

The ion-induced atomic displacement decreases rapidly as the distance, from the target atom, of the initial location of the residual atom in the surface is increased. As shown in Fig. 3, the residual atoms which are initially located within one lattice spacing from the target atom have a most probable distance of displacement of about 0.18 LS (dashed curve). The most probable displacement decreases to about 0.14 LS for atoms initially residing between 1 and 2 LS (dotted curve), to about 0.12 LS for the ones initially residing between 2 and 3 LS (dot-dashed curve), and to 0.08 LS for those initially residing between 3 and 4 LS from the target atom (dot-dot-dashed curve). The rapid decrease in the most probable displacement, as the initial atomic distance from the target atom is increased, indicates that the lattice distortion induced by static ion bombardment is quite localized in the impact region.

The magnitude of the probable displacement obtained in Fig. 3 is much smaller than the distance that an atom would move in the free space. Assuming that the primary energy of 600 eV is completely dissipated in an impact region containing 770 Ag atoms (within 4 LS from the target atom), each atom in the region would in average obtain an energy of 0.78 eV, which is equivalent to a velocity of 1200 m/s or 0.012 Å/fs. By the end of the sputtering process at ~350 fs after the primary impact, an average atom in the impact region should have traveled approximately 4.2 Å in the free space. Even we decrease the time interval by some factor to take into account of the fact that not all the atoms in the impact region are collided at the instant of the primary impact, the most probable displacement observed in Fig. 3 for the residual surface atoms in the impact region is still much smaller than the distance an average atom should have traveled in the free space by the end of atom sputtering from the surface.

A calculation of Lindemann radius [41,42] for Ag, however, indicates that during the static ion bombardment the impact region of the Ag surface may be in a state of close to melting. For Ag, the root-mean-square amplitude of vibration at the

melting point is ~0.17 LS (or 0.68 Å) for the surface atom and ~0.076 LS (or 0.31 Å) for the bulk [43]. Combining the Lindemann radius and the most probable distances of displacement obtained above with the result from Fig. 2 reveals that although the atomic movement induced in the impact region by the static ion beam may be substantial compared to the mean vibrational amplitude at melting, the lattice structure of the surface is not severely distorted in the sub-ps time range. It appears that in the time range in which sputtering takes place, the movement of atoms is limited to the spheres close to the initial lattice sites of the atoms such that the initial crystal order is retained to some extent.

It is striking that under energetic ion bombardment the lattice structure of the surface is not severely disrupted in the time range of this study. Even the atoms in the area near the impact point are mostly displaced by a distance of much less than half of the bond length in the bulk. Results from tracing individual scattering trajectories using a time-exposure representation of the collision cascade [44] show that, except for a very small number of ion impacts which result in sputtering of a large number of atoms, the surface is mostly relatively intact during static ion bombardment. The retention of crystal order during energetic ion bombardment is not mainly due to the impinging ions undergoing channeling as they penetrate the surface. Cascade analysis shows that the retention can be attributed to the fact that in each collision the interaction between the incident ion and the surface atom is brief and the scattering cross section is small that most of the atoms nearby may not have enough time to respond to the disturbance before the ion moves on. The weak bonding between Ag atoms, which results in the localization of the structural disturbance in a very small region along the ion trajectory, may also contribute to the observed extent of structural disruption by the static ion beam.

The degree of the ion-induced structural disturbance in the surface is sensitive to the property of the impinging ion. The effect of the ion size on the structural disturbance in the surface can be investigated by calculating the displacement distribution of the atoms remaining in the surface after it is bombarded by ions of different masses. Presented in Fig. 4 are the normalized distributions of the atomic displacements from the lattice sites for the atoms which remain in the Ag{1 0 0} surface after ion bombardment and are initially located within 4 LS from the target atom. As shown in the figure, similar distribution profiles are obtained for the surface bombarded by Ne^+, Ar^+, and Kr^+ ions, respectively. The most probable distance of displacement, however, varies with the size of the ion. The surface structure is less disturbed by Ne^+ than by Ar^+ ions. The most probable displacement is ~0.07 LS for Ne^+ ion bombardment and ~0.10 LS for Kr^+. Furthermore, this displacement is not directly proportional to either the mass or the momentum of the ion impinging on the surface. Our calculations show that although the ion momentum is increased by a factor of 2.0 as the incident ion is

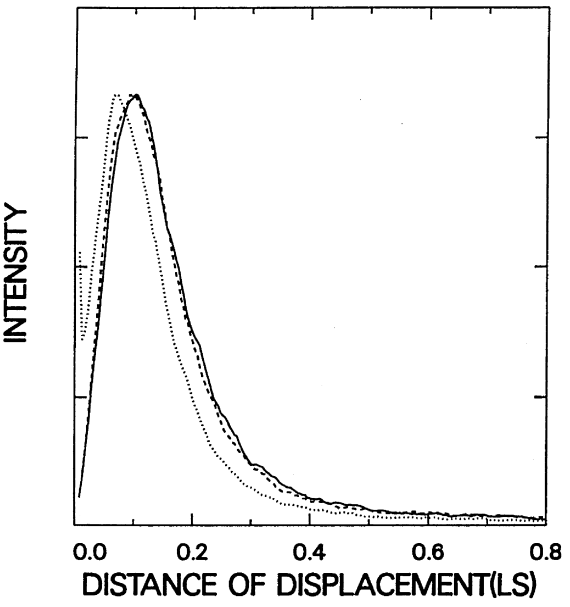

Fig. 4. Displacement distributions of the atoms remaining in the Ag{1 0 0} surface after the surface is bombarded by Kr^+ (solid curve), Ar^+ (dashed curve), and Ne^+ (dotted curve) ions, respectively, of 600 eV energy. The distributions are comprised of the effects of 100 individual ion impacts distributed uniformly in an impact zone of irreducible surface symmetry. Only the distances of displacement of the atoms initially residing within 4 LS from the target atom are included.

changed from Ne^+ to Kr^+, the most probable displacement is enlarged by a factor of 1.4 only.

The effect of the energy of the impinging ion on the extent of the structural disturbance it introduces in the surface is also examined. The displacement distributions of the atoms remaining in the Ag{1 0 0} surface after it is bombarded by the Ar^+ ions of different energies are presented in Fig. 5. The degree of structural disturbance is shown to not increase monotonously with the ion energy in the energy range between 200 eV and 4 keV. For an incident energy of 200 eV, the maximum intensity appears at ~0.0 LS. It indicates that a significant number of the surface atoms residing within the impact region of 4 LS from the target atom are not displaced from their lattice sites during bombardment of the 200 eV Ar^+ ions. For those surface atoms which are displaced at this ion energy, the most probable distance of displacement is about 0.03 LS. The crystal order becomes more disturbed as the ion energy is increased from 200 to 600 eV. Further increase of the ion energy to 1 keV does not significantly aggravate the structural destruction in the impact region. However, the intensity in the large-distance tail of the curve is slightly higher for the 1 keV ion incidence than for the 600 eV incidence, indicating that for 1 keV Ar^+ ion bombardment, the surface structure in the impact region is more disturbed.

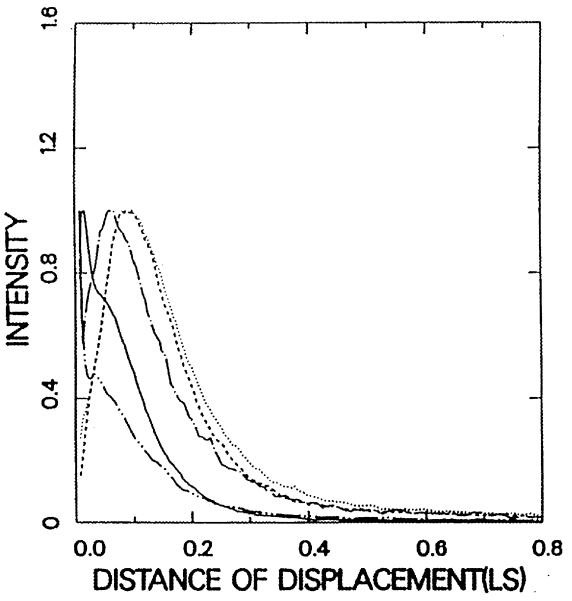

Fig. 5. Displacement distributions of the atoms remaining in the Ag{1 0 0} surface after the surface is bombarded by Ar^+ ions of 200 eV (solid curve), 600 eV (dashed curve), 1 keV (dotted curve), 2 keV (dot-dashed curve), and 4 keV (dot-dot-dashed curve) energy, respectively. The distributions are comprised of the effects of 100 individual ion impacts distributed uniformly in an impact zone of irreducible surface symmetry. Only the distances of displacement of the atoms initially residing within 4 LS from the target atom are included.

A further increase of the ion energy to 2 keV results in a decrease in the most probable distance of displacement. It changes from 0.09 to 0.06 LS as the ion energy is varied from 1 to 2 keV. Structural disturbance in the impact region of 4 LS from the target atom diminishes further as the ion energy is increased to 4 keV. The observed variation in the degree of structural disturbance with the ion bombarding energy may be related to the change in the interaction duration between the colliding partners and in the scattering cross section. At high ion energies when more momentum is available for deposition to the surface, the interaction time and the scattering cross section are both decreased. The high-energy ions, with an angle of incidence in this case parallel to the bulk channel, also tend to penetrate more into the solid that the low-energy ones. Consequently, the structural disturbance which may be generated by dissipation of more momentum in the surface at higher ion energies is counterbalanced by the effects of the shorter interaction time and the smaller scattering cross section. The atomic motion in the upper atomic layers of the surface is thus not effectively induced. It is worthy to stress that the most probable displacement shown in Fig. 5 is only for the atoms located within an impact region of 4 LS from the target atom. The magnitude of this displacement may vary with the volume of the impact region selected.

A quantitative description of surface damage may be useful in predicting the optimum conditions for the sputtering treatment and for the ion-beam lithography used in the materials processing [45]. To quantify the extent of the ion-induced structural destruction in the surface requires a detailed study of the final state of all the collision cascades developed due to ion impacts. In this

work, instead of studying the final state of the cascades, the state of the cascades at the end of the sputtering process is studied. The average distance of displacement of the residual surface atoms from their initial lattice sites is first calculated. The surface disorder induced by ion bombardment is then evaluated as a function of the initial distance of the surface atom from the target atom. As shown in Fig. 6, the average distance of displacement for the atoms remaining in the surface after static ion bombardment decreases rapidly as the initial distance of the residual atom from the target atom is increased. For the 1 keV Ar^+ ion impinging on the Ag{1 0 0} surface, the average displacement of the target atom which survives the primary impact is as large as 0.88 LS. Atoms initially residing in the first neighboring shell of the target atom are displaced in average by a distance of about 0.5 LS. The average distance of displacement further decreases to less than 0.2 LS for the surface atoms initially residing at distances of more than 3 LS from the target atom. It is estimated by extrapolation that the average displacement will approach zero for the atoms located at a distance of about 7 LS from the target atom.

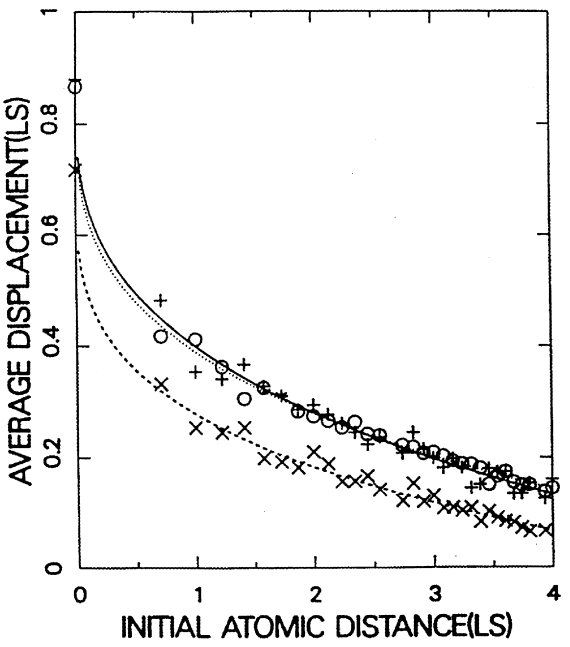

Fig. 6. Dependence of the average atomic displacement from the lattice site on the initial distance of the residual surface atom from the target atom after the Ag surfaces are bombarded by Ar^+ ions of 1 keV energy. The solid line represents the least-squares best-fit curve for the average displacement calculated from the {1 0 0} surface; the dashed line the best-fit curve for the one calculated from the {1 1 0} surface; and the dotted line the one from the {1 1 1} surface. These lines are comprised of the effects of at least 100 individual ion impacts.

Also presented in Fig. 6 is the dependence of the average displacement on the initial distance of the residual atom from the target atom for ions impinging upon the Ag{1 1 0} and Ag{1 1 1} surfaces. The extent of the ion-induced structural disturbance in the surface is found to vary with the face of the crystal exposed to the bombarding ions. Under the same ion bombardment condition, atoms in the {1 1 0} surface are less displaced than those in the {1 0 0} surface. Fig. 6 shows that the atoms initially residing in the first neighboring shell of the target atom in the {1 1 0} surface are displaced in average by a distance of about 25% (or about 0.2 LS) less than those in the {1 0 0} surface. The difference in the average displacement of the residual atoms between these two surfaces increases to about 50% for the atoms initially residing at 4 LS from the target atom. For the case of ion bombardment on the {1 1 1} surface, the dependence of the average displacement on the initial atomic distance is very close to that observed for the bombardment on the {1 0 0} surface. It should be pointed out that the average atomic displacement measured experimentally may be less than what is shown in the figure, since the hopping of the surface atom from one lattice site to another is treated in this calculation as a displacement from the initial atomic location.

The smaller average displacement of the atoms in the {1 1 0} surface, as compared with that observed in the {1 0 0} and {1 1 1} surfaces, may be associated with the number of the atoms per unit surface area exposed to the incident ion beam. As viewed by the ions impinging normal to the surface, the densities of the atoms exposed are 0.240, 0.169, and 0.231 atoms/$Å^2$ for the {1 0 0}, {1 1 0} and {1 1 1} surfaces, respectively [46]. The average displacement of the surface atoms due to ion bombardment is thus greater for surfaces with higher atomic densities.

4. Conclusions

The present study shows that, although the atomic movement induced in the surface by the static ion beam may be substantial compared to the mean vibrational amplitude at melting, the lattice structure of the surface is not severely distorted in the time range in which sputtering takes place. Even in the impact region of 4 LS from the target atom, most surface atoms are displaced from their initial lattice sites by only a fraction of the equilibrium bond length in the solid. The path of the atoms sputtered late in the collision cascade from the second atomic layer of the surface is thus mostly confined by the fourfold hole formed by the first-layer atoms residing close to their initial positions. At an ion bombarding energy of between 600 eV and 1 keV, the most probable distance of displacement for the atoms in the impact region is about one eighth of the equilibrium Ag–Ag bond length in the bulk, although the average distance of displacement is by a factor of $\sim$2.5 larger. The most probable displacement does not increase monotonously with the bombarding energy of the incident ions. The degree of surface damage is related to the face of the crystal exposed to the ion bombardment. Surfaces with an open structure tend to be less disrupted than those with a higher surface atomic density.

Our results reveal that, although the ''mega-event'' [24,25] induced by the ion impacts may be important under some specific conditions of ion incidence, these events are rare and do not contribute significantly to the total amount of surface damage created by the static keV ion bombardment. It is thus possible to characterize the geometric structure of the surface using the static secondary ion mass spectrometry (SIMS) [47,48]. Results of our studies on the dependence of the average displacement upon the initial atomic distance from the target atom also reveal that the ion-induced structural disturbance is very localized. Assuming that the crystal order of the Ag surface is destroyed when the average displacement is more than a quarter of the equilibrium bond length in the bulk, the displacement dependence obtained in this study implies that a static SIMS experiment using the 1 keV Ar^+ ions impinging on the Ag surface has to be performed with an ion fluence of less than $\sim$1500 nA s/cm^2 for better determining the surface bonding geometry.

Furthermore, this study shows that the surface under the single-ion impacts retains to some extent the initial lattice structural order near the end of the sputtering process of particles from the surface. Since the kinetic energy of ejection is small near the end of particle sputtering, surface structural studies by the angle-resolved SIMS [49] may thus be performed by collecting sputtered particles with kinetic energies of less than 20 eV [50]. The advantages of collecting low-energy particles of sputtering from the surface for surface characterization include an enhanced detection sensitivity, since the sputter yield at energies of $\sim$5 eV may be as large as an order of magnitude [51] higher than that at $\sim$20 eV, and a less disturbance on the surface being analyzed, since a smaller incident ion flux can be employed.

Acknowledgements

This work was supported by ROC National Science Council and Chinese Petroleum Corporation. The author wishes to thank Bih-Yaw Jin for helpful discussions. The contribution of the reviewers' comments to this work is also gratefully acknowledged.

References

[1] K. Gamo, Nucl. Instr. and Meth. B 121 (1997) 464.
[2] F.A. Smidt, Int. Mat. Rev. 35 (1990) 61.
[3] W.H. Brunger, L.-M. Buchmann, M.A. Torkler, W. Finkelstein, J. Vac. Sci. Technol. B 12 (1994) 3547.
[4] I.W. Rangelow, P. Hudek, F. Shi, Vacuum 46 (1995) 1361.
[5] S.Y. Chou, P.R. Krauses, P.J. Renstrom, J. Vac. Sci. Technol. B 14 (1996) 4129.
[6] B.D. Weaver, D.R. Frankl, R. Blumenthal, N. Winograd, Surf. Sci. 222 (1989) 464.
[7] A.H. Al-Bayati, K.G. Orrman-Rossiter, D.G. Armour, Surf. Sci. 249 (1991) 293.
[8] S.A. Larson, L.L. Lauderback, Surf. Sci. 254 (1991) 161.
[9] Y. Kido, I. Konomi, M. Kakeno, K. Yamada, K. Dohmae, J. Kawamoto, Nucl. Instr. and Meth. B 15 (1986) 42.
[10] I. Konomi, A. Kawano, Y. Kido, Surf. Sci. 207 (1989) 427.

[11] Th. Michely, G. Comsa, Phys. Rev. B 44 (1991) 8411.
[12] C. Teichert, M. Hohage, Th. Michely, G. Comsa, Phys. Rev. Lett. 72 (1994) 1682.
[13] M. Ritter, M. Stindtmann, M. Farle, K. Baberschke, Surf. Sci. 348 (1996) 243.
[14] I.H. Wilson, N.J. Zheng, U. Knipping, I.S.T. Tsong, Phys. Rev. B 38 (1988) 8444.
[15] T. Michely, K.H. Besocke, G. Comsa, Surf. Sci. 230 (1990) L135.
[16] J.C. Girard, Y. Samson, S. Gauthier, S. Rousset, J. Klein, Surf. Sci. 302 (1994) 73.
[17] U. Bangert, P.J. Goodhew, C. Jeynes, I.H. Wilson, J. Phys. D 19 (1986) 589.
[18] M. Ghaly, R.S. Averback, T. Diaz de la Rubia, Nucl. Instr. and Meth. B 102 (1995) 51.
[19] D.J. Eaglesham, P.A. Stolk, H.-J. Gossmann, T.E. Haynes, J.M. Poate, Nucl. Instr. and Meth. B 106 (1995) 191.
[20] A. Caballero, J.P. Espinos, A. Fernandez, D. Leinen, A.R. Gonzalez-Elipe, Nucl. Instr. and Meth. B 97 (1995) 397.
[21] P. Rabinzohn, G. Gautherin, B. Agius, C. Cohen, J. Electrochem. Soc. 131 (1984) 905.
[22] B.S. Swartzentruber, C.M. Matzke, D.L. Kendall, J.E. Houston, Surf. Sci. 329 (1995) 83.
[23] D. Pedersen, R.A. Weller, M.R. Weller, V.J. Montemayor, J.C. Banks, J.A. Knapp, Nucl. Instr. and Meth. B 117 (1996) 170.
[24] R. Smith, D.E. Harrison Jr., Phys. Rev. B 40 (1989) 2090.
[25] R.P. Webb, D.E. Harrison Jr., Phys. Rev. Lett. 50 (1983) 1478.
[26] C. Teichert, M. Hohage, T.H. Michely, G. Comsa, Phys. Rev. Lett. 72 (1994) 1682.
[27] T. Michely, C. Teichert, Phys. Rev. B 50 (1994) 11156.
[28] T. Li, B.V. King, R.J. MacDonald, G.F. Cotterill, D.J. O'Connor, Q. Yang, Surf. Sci. 312 (1994) 399.
[29] R. Coratger, A. Claverie, A. Chahboun, V. Landry, F. Ajustron, J. Beauvillain, Surf. Sci. 262 (1992) 208.
[30] G.M. Shed, P.E. Russell, J. Vac. Sci. Technol. A 9 (1991) 1261.
[31] H.J.W. Zandvliet, H.B. Elswijk, E.J. van Loenen, I.S.T. Tsong, Phys. Rev. B 46 (1992) 7581.
[32] H.M. Urbassek, Nucl. Instr. and Meth. B 122 (1997) 427.
[33] D.E. Harrison Jr., Crit. Rev. Solid State Mat. Sci. 14 (1988) S1.
[34] C.-C. Chang, N. Winograd, B.J. Garrison, Surf. Sci. 202 (1988) 309.
[35] G. Moliere, Z. Naturf. A 2 (1947) 133.
[36] O.B. Firsov, JETP Trans Sov. Phys. 6 (1958) 534.
[37] D.J. O'Connor, J.P. Biersack, Nucl. Instr. and Meth. B 15 (1986) 14.
[38] C.-C. Chang, Surf. and Interf. Anal. 15 (1990) 79.
[39] C.-C. Chang, N. Winograd, Phys. Rev. B 39 (1989) 3467.
[40] C.-C. Chang, Formosan Sci. 46 (1993) 9.
[41] H. Bottger, Principles of the Theory of Lattice Dynamics, ch. 1, Akademie Verlag, Berlin, 1983.
[42] K. Ishizaki, I.L. Spain, P. Bolsaitis, J. Chem. Phys. 63 (1975) 1401.
[43] For Debye temperatures, see J.M. Morabito, Jr., R.F. Steiger, G.A. Somorjai, Phys. Rev. 179 (1969) 638.
[44] C.-C. Chang, Phys. Rev. B 48 (1993) 12399.
[45] T. Nishihara, M. Shinohara, O. Ishiyama, F. Ohtani, M. Yoshimoto, T. Maeda, H. Koinuma, J. Electron. Mat. 25 (1996) 667.
[46] For ions incident normal to the {1 0 0} and {1 1 0} surfaces, all the atoms located deeper than the second-layer are blocked from the view of the bombarding ions by the top two surface layers. Also, since the interlayer spacing in the {1 1 1} surface is quite large, we assume in the calculation of its atomic density that the exposure of the third-layer atoms does not significantly affect the resulting ion-induced surface disorder.
[47] C.-C. Chang, N. Winograd, Surf. Sci. 230 (1990) 27.
[48] N. Winograd, C.-C. Chang, Phys. Rev. Lett. 62 (1989) 2568.
[49] N. Winograd, B.J. Garrison, D.E. Harrison Jr., Phys. Rev. Lett. 41 (1978) 1120.
[50] C.-C. Chang, J.-Y. Hsieh, submitted to J. Chem. Phys.
[51] M. Szymonski, Nucl. Instr. and Meth. 194 (1982) 523.